Impact Assessment of Simulated Doppler Wind Lidars with a Multivariate Variational Assimilation in the Tropics

NEDJELJKA ŽAGAR

University of Ljubljana, Ljubljana, Slovenia, and National Center for Atmospheric Research, Boulder, Colorado

AD STOFFELEN AND GERT-JAN MARSEILLE

Royal Netherlands Meteorological Institute, De Bilt, Netherlands

CHRISTOPHE ACCADIA AND PETER SCHLÜSSEL

European Organisation for the Exploitation of Meteorological Satellites, Darmstadt, Germany

(Manuscript received 2 August 2007, in final form 7 November 2007)

ABSTRACT

This paper deals with the dynamical aspect of variational data assimilation in the tropics and the role of the background-error covariances in the observing system simulation experiments for the tropics. The study uses a model that describes the horizontal structure of the potential temperature and wind fields in regions of deep tropical convection. The assimilation method is three- and four-dimensional variational data assimilation. The background-error covariance model for the assimilation is a multivariate model that includes the mass–wind couplings representative of equatorial inertio-gravity modes and equatorial Kelvin and mixed Rossby–gravity modes in addition to those representative of balanced equatorial Rossby waves. Spectra of the background errors based on these waves are derived from the tropical forecast errors of the European Centre for Medium-Range Weather Forecasts (ECMWF) model.

Tropical mass–wind (im)balances are illustrated by studying the potential impact of the spaceborne Doppler wind lidar (DWL) Atmospheric Dynamic Mission (ADM)-Aeolus, which measures horizontal line-of-sight (LOS) wind components. Several scenarios with two DWLs of ADM-Aeolus type are compared under different flow conditions and using different assumptions about the quality of the background-error covariances.

Results of three-dimensional variational data assimilation (3DVAR) illustrate the inefficiency of multivariate assimilation in the tropics. The consequence for the assimilation of LOS winds is that the missing part of the wind vector can hardly be reconstructed from the mass-field observations and applied balances as in the case of the midlatitudes.

Results of four-dimensional variational data assimilation (4DVAR) show that for large-scale tropical conditions and using reliable background-error statistics, differences among various DWL scenarios are not large. As the background-error covariances becomes less reliable, horizontal scales become smaller and the flow becomes less zonal, the importance of obtaining information about the wind vector increases. The added value of another DWL satellite increases as the quality of the background-error covariances deteriorates and it can be more than twice as large as in the case of reliable covariances.

1. Introduction

A lack of direct observations of wind profile measurements over a significant part of the earth has been recognized as the main missing component of the current operational observing system (e.g., Baker et al. 1995; World Meteorological Organization 2000). The problem is most severe in the tropics, where wind field information is also more important than mass information for the atmospheric dynamics and initialization of the numerical weather prediction (NWP) models (e.g., Gordon et al. 1972; Atlas 1997; Žagar et al. 2004b, hereafter ŽGK). As a consequence, tropical (re)analy-

Corresponding author address: Nedjeljka Žagar, National Center for Atmospheric Research, P.O. Box 3000, Boulder, CO 80307-3000.
E-mail: nzagar@ucar.edu

DOI: 10.1175/2007MWR2335.1

ses are dominated by background information (NWP model; e.g., Kistler et al. 2001). The importance of using a reliable estimate of the background-field errors in data assimilation can therefore hardly be overestimated. This paper is concerned with the background-error estimates for tropical data assimilation and the role of these errors in studies used to design future observing systems.

A majority of global operational NWP assimilation systems utilizes three- and four-dimensional variational data assimilation (3DVAR, 4DVAR) procedures (Rabier 2005). In NWP models, the background-error variances are dominated by errors in the storm-track regions in the midlatitudes. Variances in the tropics are small, especially variances in the mass-field variables. The background-error correlations are stationary in 3DVAR and at the start of the 4DVAR assimilation time window. These correlations are modeled; the role of the covariance model is to spread the impact of observations in the model space and to impose the mass–wind balance (e.g., Lorenc 2003). Globally, the balance is achieved by estimating the balanced wind and geopotential fields by solving the nonlinear balance equation (Fisher 2003). In the tropics, the application of the nonlinear balance provides very little information about the balanced wind field; in other words, the assimilation behaves as if the analysis was done in a univariate fashion.

More recently, an attempt has been made toward a multivariate tropical assimilation procedure (ŽGK) based on the theory for equatorial linear waves coupled to convection. Equatorial waves represent a significant portion of the large-scale variability in the tropics (e.g., Wheeler and Kiladis 1999, and references therein) on scales of interest for NWP, and their accurate analysis should also benefit medium- and extended-range predictability in the extratropics (e.g., Ferranti et al. 1990).

The background-error covariance model, developed in ŽGK, includes the mass–wind couplings representative of equatorial inertio-gravity (EIG) modes, equatorial Kelvin and mixed Rossby–gravity (MRG) modes, in addition to the balanced equatorial Rossby (ER) motions. The relative contributions of various tropical motions to the total error variance have been studied by projecting the background errors used in the European Centre for Medium-Range Weather Forecasts (ECMWF) model onto the equatorially trapped subset of linear tropical waves (Žagar et al. 2005, 2007). It was found in these studies that, on average, about 70% of the short-range forecast errors in the tropics can be represented by equatorial wave solutions as derived by Matsuno (1966).

In the present study, we apply the background-error spectra derived from the ECMWF model to look more closely into the dynamical properties of the tropical data assimilation. We illustrate the univariate nature of the mass–wind coupling in the tropics by using the multivariate covariance model, and we compare the impacts of mass and wind observations in the tropical assimilation using these "realistic" background-error spectra.

Mass–wind (im)balances are illustrated in the context of observing system simulation experiments (OSSE). The observing system in question is the spaceborne Doppler wind lidar (DWL), the first satellite to provide global coverage of wind profiles (Stoffelen et al. 2005b). The mission, called Atmospheric Dynamic Mission (ADM)-Aeolus, will measure the horizontal line-of-sight (LOS) wind component perpendicular to the satellite track. In the tropics, the ADM measurements are close to the zonal direction. Because of this incomplete wind information and because of the sparse horizontal sampling of measurements, spatial structures in the analysis fields emerge mainly from the background information. In particular, the meridional flow across the equator is inferred from assumed background-error covariances, which are rather uncertain, as a consequence of basic atmospheric conditions in the tropics.

The ADM mission is scheduled for launch in 2009, and the European Space Agency (ESA) is now considering the development of long-lead items necessary for a DWL mission following ADM-Aeolus. Although the European Organisation for the Exploitation of Meteorological Satellites (EUMETSAT) recently launched its first polar satellite (*MetOp-A*) in a series of three over 15 yr, a EUMETSAT expert team is already considering the next generation of polar satellites, among which is a potential ADM-Aeolus follow-on mission.

Related to these actions, several spaceborne DWL sampling scenarios were proposed in the frame of a project devoted to the Prediction Improvement for Extreme Weather (PIEW; Marseille et al. 2008). PIEW concentrated on post-ADM scenarios in the Northern Hemisphere extratropics by studying the potential of different scenarios with two DWLs to improve unsuccessful 2-day forecasts of the ECMWF model.

This study addresses the potential impact of several proposed scenarios in the tropics. However, the present paper does not aim at providing a realistic assessment of the impact of these scenarios in a full-scale NWP data assimilation system. We concentrate on dynamical aspects of assimilating various DWL scenarios with a goal of highlighting uncertainties related to the background-error term in variational data assimilation in the tropics. This study thus employs a simplified model that describes potential temperature and wind pertur-

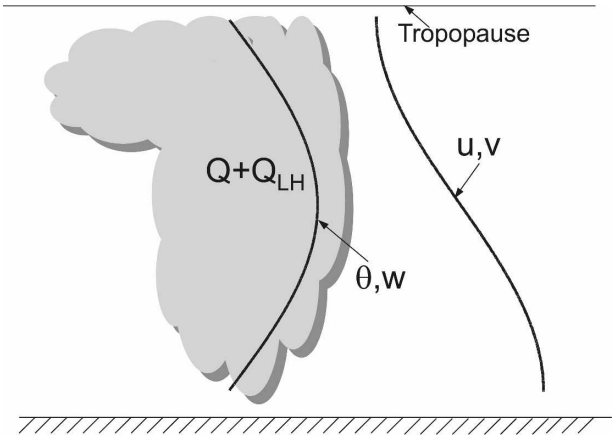

FIG. 1. Simple tropical atmosphere model as envisaged by A. Gill.

bations associated with the first baroclinic mode of the tropical atmosphere in regions of deep convection. The model details are presented in section 2, which also presents tropical data assimilation methodologies for and in relation to previous studies. Details about DWL scenarios, as well as the preparation of observations and the nature simulations, are provided in section 3. Results are discussed in section 4. Various sensitivity experiments are performed to describe the factors that are important for the impact of LOS winds. Discussion is provided in section 5; conclusions are stated in section 6.

2. Tropical data assimilation modeling

a. Numerical model

The variational analysis problem is solved for a nonlinear system including three prognostic variables: potential temperature and the two horizontal velocity components. The model equations describe the tropical atmosphere in regions of deep convection, as envisaged by Gill (1982). In convective regions, diabatic heating has a vertical profile as shown in Fig. 1: a deep structure with a peak in the midtroposphere. The heat balance in this case is maintained by vertical motion within deep cumulus convection, where updrafts within individual convective cells couple the surface layer and the upper troposphere. This forcing projects predominantly onto the first baroclinic mode; thus, the distribution of the vertical velocity is also sinusoidal in the vertical. The corresponding horizontal velocity and pressure perturbations are derivatives of this quantity and thus have opposite signs in the lower and upper troposphere. The corresponding mass-field equation describes the potential temperature perturbation (θ') at some middle level because pressure perturbation (p') is proportional to the difference in pressure between the lower and upper layer (i.e., the lower and the upper troposphere, respectively); that is, $p' = -(H_o\rho_o g\theta'/\theta_o)$. In this equation, H_o is a representative depth for the lower layer (about 5–6 km), θ_o is a representative mean potential temperature, and ρ_o, a constant, is the air density.

The continuity equation applied to the lower layer is

$$H_o\left(\frac{\partial u}{\partial x}+\frac{\partial v}{\partial y}\right)+w=0, \tag{1}$$

where w is the vertical velocity at some middle atmospheric level.

The system of prognostic equations (with primes dropped) is then the following:

$$\frac{\partial\theta}{\partial t}+u\frac{\partial\theta}{\partial x}+v\frac{\partial\theta}{\partial y}-\frac{\theta_o N^2 H_o}{g}\left(\frac{\partial u}{\partial x}+\frac{\partial v}{\partial y}\right)=Q+Q_{\mathrm{LH}}-\varepsilon_\theta\theta, \tag{2}$$

$$\frac{\partial u}{\partial t}+u\frac{\partial u}{\partial x}+v\frac{\partial u}{\partial y}-fv=\frac{gH_o}{\theta_o}\frac{\partial\theta}{\partial x}-\varepsilon_u u, \tag{3}$$

$$\frac{\partial v}{\partial t}+u\frac{\partial v}{\partial x}+v\frac{\partial v}{\partial y}+fu=\frac{gH_o}{\theta_o}\frac{\partial\theta}{\partial y}-\varepsilon_v v. \tag{4}$$

Here, N is a representative buoyancy frequency, such that $N^2=(g/\theta_o)(\partial\theta_o/\partial z)$. Total latent heating is denoted by Q_{LH}; Q stands for an additional prescribed thermal forcing. Frictional processes are parameterized by ε. Friction is used in connection with Q to balance additional mass input to the system, and it usually has a value on the order of several days. These equations apply to the lower layer. At the upper level, u, v, and p' are reversed in sign. The latent heating Q_{LH} is associated with precipitation, which can be determined by a dynamic moisture equation for total column moisture (Gill 1982).

Various solutions of the Gill model have been used to describe the horizontal structure of dynamical fields that develops in response to deep tropical heating. For example, Gill (1980) used steady-state solutions of the system with applied longwave approximation to reproduce the main large-scale features of the tropics, Heckley and Gill (1984) presented time-dependent analytical solutions to the problem of a sudden "switch-on" of heating localized around the equator, Davey and Gill (1987) looked at the moist model response to prescribed sea surface temperatures, and Davey (1989) applied the moist system to surface temperature forcing for studying the Madden–Julian oscillation.

b. Tropical data assimilation approach

The numerical solution of Eqs. (2)–(4) closely follows that of the shallow-water equations described in

Žagar et al. (2004a). Prognostic variables are discretized using a spectral transform formulation using Fourier series. The spectral approach has a distinct advantage for variational data assimilation because the Fourier transform is a self-adjoint operator. The adjoint version of the model needs to be applied in the minimization of the following tropical distance (cost) function (J), shown below:

$$J(\chi) = J_b + J_o = \frac{1}{2}\chi^{\mathrm{T}}\mathbf{E}^{-1}\chi + \frac{1}{2}\sum_{n=1}^{K}\left[\mathbf{y}_n - H(\mathbf{x}^b + L^{-1}\chi_n)\right]^{\mathrm{T}}\mathbf{R}^{-1}\left[\mathbf{y}_n - H(\mathbf{x}^b + L^{-1}\chi_n)\right]. \quad (5)$$

The cost function J consists of the distance to a background model (J_b) and the distance to the observations measured by J_o. The observation vector at time n is denoted by $\mathbf{y}_n$, and observations are distributed among K different times. The model state vector $\mathbf{x}$ is defined as $\mathbf{x} = (\theta, u, v)^{\mathrm{T}}$ and the background state is denoted by $\mathbf{x}^b$. The operator H generates the model equivalents of observations at the observations points. The observation error covariance matrix is denoted by $\mathbf{R}$, and the background-error covariance matrix, normally denoted by $\mathbf{B}$, appears in the J_b term of Eq. (5) as $\mathbf{E}$, an identity matrix. This is because the control variable for minimization χ is formulated so that the $LL^{-1} = \mathbf{B}$ (i.e., the $\mathbf{B}$ matrix is made diagonal). The basic idea behind the present approach, originally proposed by Daley (1993) and developed for the variational assimilation in ŽGK, is based on the representation of the tropical analysis increments in terms of linear waves (ER, EIG, MRG, and Kelvin waves) on the equatorial β plane.

A sequence of linear operators that transforms the analysis increment $\delta\mathbf{x}$ to the new control variable χ and thereby makes the background-error covariance matrix diagonal is the following:

$$\chi = L\delta\mathbf{x} = TDP_yF_xF^{-1}\delta\mathbf{x}. \quad (6)$$

Here F^{-1} is the inverse Fourier transform to obtain assimilation increments in gridpoint space and F_x is the direct Fourier transform in the zonal direction. The projection on the meridionally dependent part of the equatorial eigenmodes in gridpoint space is denoted by P_y, and D stands for the normalization by the spectral variance density. The operator T summarizes the means of truncation in the model (i.e., Fourier truncation, elliptic truncation, and frequency cutoff). Details of the derivation of Eq. (6) are provided in ŽGK. At the end of the minimization, an inverse of (6) is applied to produce analysis increments that are added to the background field to produce the analysis field ($\mathbf{x}^a = \mathbf{x}^b + \delta\mathbf{x}$) for the subsequent model integration.

c. Background-error variances

The relative importance of various tropical motions included in the assimilation is specified by the operator D, the spectral variance density. This operator normalizes each wave component of the control vector as a function of the zonal wavenumber k, a meridional mode number n (the order the Hermite polynomial), and the wave type (there are six types altogether: eastward- and westward-propagating EIG, Kelvin, eastward- and westward-propagating MRG, and equatorial Rossby modes). This is the last operation in Eq. (6), which transforms the now-diagonal background-error covariance matrix to the identity matrix [$\mathbf{E}$ in Eq. (5)].

The variance spectrum was derived from a more recent dataset used in the ECMWF model (Žagar et al. 2007) by applying the methodology described in Žagar et al. (2005). Figure 2 displays the resulting spectral error-variance densities at a model level close to 500 hPa. In this case, about 43% of the background-error variance is represented in terms of ER modes, westward- and eastward-propagating EIG modes (WEIG and EEIG, respectively) together make 39% of the error variance, 8% belongs to the Kelvin waves, and about 10% of the variance pertains to the MRG modes. Horizontal correlations associated with the spectra shown in Fig. 2 can be illustrated by single-observation experiments, which appear very similar to those presented in Žagar et al. (2005, Figs. 9–11) for an earlier

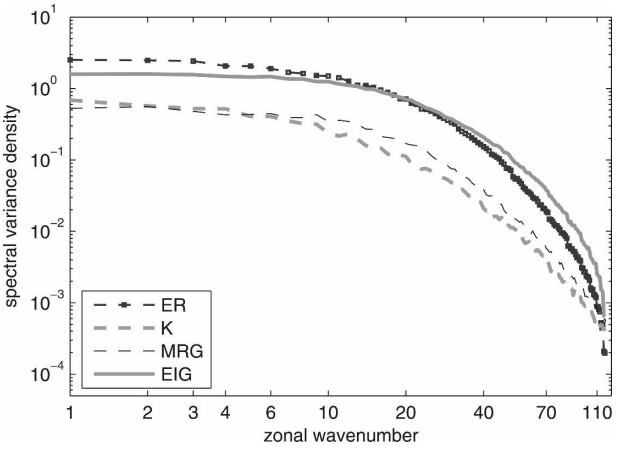

FIG. 2. Spectral variance density in ER, Kelvin (K), MRG, and EIG modes at the ECMWF model level close to 500 hPa, as a function of a zonal wavenumber.

TABLE 1. Summary of satellite scenarios considered in the paper. The number of profiles refers to the number of observations collected during 12 h within the tropical belt 33°S–33°N, used for the model domain.

Scenario	Inclination angles	Azimuth at equator	No. of profiles	Experiment label
ADM-Aeolus	97.2°	7°	570	Aeolus
Tandem-Aeolus	97.2°, 97.2°	7°, 7°	1130	Tandem
Dual-inclination	97.2°, 70°	7°, 240°	1238	Dual-incl
Dual-perspective	97.2°, 97.2°	52°, 142°	1138	Los2-DD
Reduced dual-perspective	97.2°, 97.2°	52°, 142°	571	Los2-D

dataset. In the derivation of the background-error covariances, all zonal modes allowed by the elliptic truncation criterion were included, but only 10 (out of 23) meridional modes were allowed because of a limited domain (20°S–20°N) and the orthogonality criterion.

d. Relation to the previous work

Several important differences exist between the previous paper (Žagar 2004, hereafter Ž04) that studied the potential of LOS winds in the tropics and the present study.

The model used in the previous study was based on shallow-water equations. With a system based on the geopotential height (h) of the free fluid surface, an average fluid depth (h_o, also interpreted as the equivalent depth) defines the phase speed (c) of fastest waves via $c = \sqrt{gh_o}$. Because characteristic values for the phase speed of the equatorial waves coupled to convection are around 15 m s^{-1} (Wheeler and Kiladis 1999), a time window for four-dimensional data assimilation was set at 48 h to allow the information transfer to take place between the mass and wind fields in 4DVAR (Ž04). In the present model, the gravity wave speed is defined by the lower layer depth (the height of the tropopause for the first baroclinic mode is at πH_o) and the static stability; for typical values c is about 60 m s^{-1}. A 12-h window, usually used in NWP models, is now sufficiently long for the 4DVAR dynamics.

Another important difference between the present model and the one used in Ž04 is the background-error variance spectrum, which in the earlier study was modeled analytically. The spectrum included only the lowest two meridional modes of WEIG; no EEIG waves were allowed in the spectrum and a twice smaller number of meridional modes of ER waves was included. The model also considered only the largest scales, and the amount of divergence in the simulated flow was small. As shown in the next section, the consequences of using more realistic background-error spectra are seen in a reduced efficiency of the assimilation system, compared to that in Ž04, to spread assimilated LOS wind information to unobserved variables.

3. Implementation of the tropical OSSE system

a. Observations: DWL scenarios

ADM-Aeolus and four additional scenarios involving two satellites are studied. Table 1 summarizes their main characteristics in terms of orbit inclination, observation azimuth at the equator, and number of available observations; some further details can be found in PIEW. In each case, a scenario consists of the ADM-Aeolus track plus an additional DWL instrument of Aeolus type in the same or a different orbit. Three of the four scenarios were proposed in PIEW. A fourth scenario is included for comparison reasons as explained below.

Measurement locations for four scenarios, together with their LOS directions during 6 h, are shown in Fig. 3. As seen in this figure, the global surface coverage is maximized for the tandem-Aeolus scenario. In this scenario, two satellites share the same orbit plane but they are separated in the orbit phase by 180° (Fig. 3a). In case of the dual-inclination scenario, two Aeolus-type satellites operate in separate orbit planes and with different inclination angles (Fig. 3b). The dual-inclination scenario was prepared in PIEW for targeting the storm-track regions to maximize the coverage close to 70° north and south latitude. The dual-perspective scenario measures wind vectors in the Aeolus orbit (Fig. 3c); the reduced dual-perspective scenario provides the same observations but the sampling is only half of that in the dual-perspective scenario (Fig. 3d). Wind measurements take place over a 50-km range, followed by 150 km without measurements. In this way, a wind vector projection along the direction of the line of sight is provided every 28 s (Stoffelen et al. 2005b). In the reduced dual-perspective scenario, two LOS measurements perpendicular to each other are provided every 56 s.

Figure 3 also shows that the inclination angle of 97°, defined here as an angle between a line of sight and the y axis (north), makes the ADM measurements in the tropics nearly zonal. On average, the tropics receive a smaller percentage of profiles than the midlatitudes;

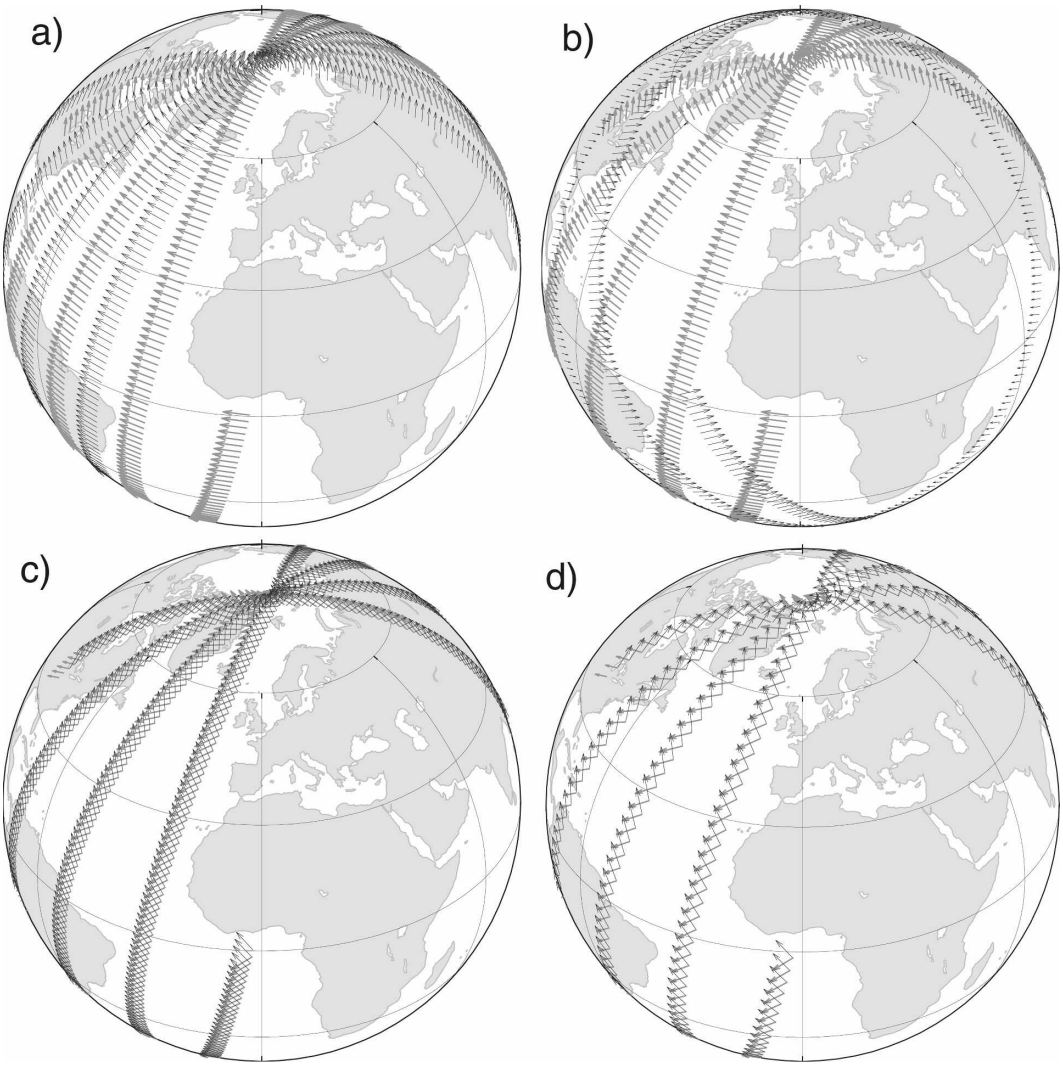

FIG. 3. Observation coverage of the globe for various DWL scenarios during 12 h: (a) tandem-Aeolus, (b) dual-inclination, (c) dual-perspective, and (d) reduced dual-perspective scenarios. Arrows start at the locations of the measurements and point along the line of sight. Thick gray arrows correspond to the Aeolus orbit; thin black arrows denote the orbit of the second satellite.

about one-third of the measurements cover about one-half of the atmosphere. A smaller inclination angle of the second satellite in the dual-inclination scenario means that in this case the tropics receive relatively more observations than in the case of the tandem-Aeolus and dual-perspective scenarios (about 10% more). Another difference between the tandem and dual-inclination scenarios is that the latter also provides partial information about meridional wind components. The dual-perspective scenarios provide the wind vector at the expense of zonal coverage.

b. Definition of nature and observations

Assimilation experiments are of "identical twin" OSSE type. In this approach, a "nature run" is performed first, creating an artificial history of the atmosphere by numerical integration of the same model used for later assimilation experiments. Simulated observations are generated from the nature run by adding random error (from a distribution of zero mean and variance equal to the background-error variance) to the historical values for the potential temperature field and the two wind components. Hereafter, assimilation is conducted with the same model and with simulated data at times and locations corresponding to the simulated patterns of DWL observations. The observation operator for LOS winds interpolates the model wind to positions of DWL measurements and calculates the model equivalent of the LOS component.

Temperature observations are assumed to have been

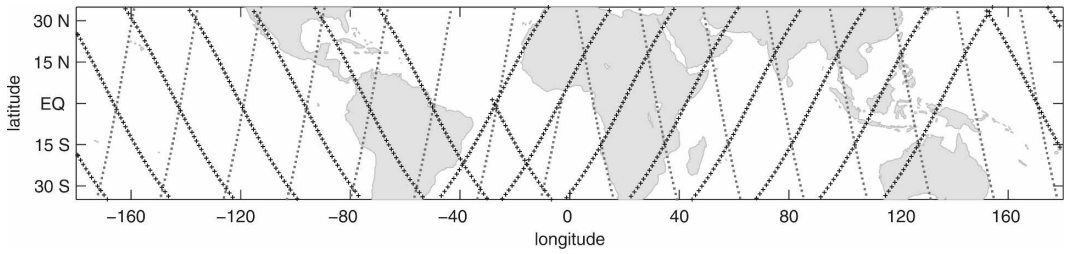

FIG. 4. The model domain used for variational assimilation with the observation coverage by the dual-inclination scenario during 6 h. Gray squares represent the observation locations of ADM-Aeolus. Black pluses correspond to the second satellite, which has an inclination angle of 70°.

taken at the same locations as LOS winds. In more realistic experiments, one should take into account the fact that there are many more temperature measurements available from satellites. However, in the present study we compare the dynamics of various observation types in a multivariate assimilation system; it is thus suitable to assimilate temperature data at the locations of LOS winds. Tests were performed to check that adding more locations with temperature observations does not change our conclusions concerning the relative impact of various scenarios and the role and the background-error covariances.

The modeling domain is shown in Fig. 4. The domain is a channel between 33°S and 33°N and the resolution is 1° (360 × 67 grid points). Periodic boundary conditions are applied in the zonal direction. As presented below, observations are simulated and assimilated over the whole model domain; however, verification of the analysis outputs is carried out within the tropical belt between 20°S and 20°N.

The amount of DWL observations is not large; LOS winds simulated from two DWLs in 12 h provide about 5% of the number of degrees of freedom needed for a variable on the selected tropical domain (Fig. 4). Observations are nearly homogeneously distributed throughout the 12-h window. With the time step of 180 s used in all experiments and the measurements taken every 28 s, there are between 1 and 14 LOS wind components available for assimilation from two DWLs at any particular time step. The number of time steps with observations in 4DVAR varies between 102 (Aeolus) and 121 (tandem-Aeolus scenario). For 3DVAR experiments, all observations accumulated in the 12-h period are assumed valid at a single time instant. This is an unrealistic assumption, but it serves our purpose to illustrate the impact of the background-error covariance propagation in 4DVAR in comparison to multivariate relationships in 3DVAR using the same amount of observations.

Estimated background-error variances are spectral variance densities. Values of the background-error standard deviations in the gridpoint space are obtained by carrying out a "randomization experiment" (Fisher and Courtier 1995; Andersson et al. 1999), which computes effective variances of the $\mathbf{B}$ matrix in gridpoint space by making use of the applied J_b formulation. Background-error variances are estimated by the following equation:

$$\mathbf{H}\tilde{\mathbf{B}}\mathbf{H}^{\mathrm{T}} = \frac{1}{N}\sum_{i=1}^{N}(\mathbf{H}F^{-1}L^{-1}\zeta_i)(\mathbf{H}F^{-1}L^{-1}\zeta_i)^{\mathrm{T}}, \qquad (7)$$

where $\mathbf{H}$ represents the linearized observation operator. In Eq. (7), ζ is a random vector drawn from a Gaussian distribution of zero mean and unit variance in space of the control variable χ. The number of random samples N is taken to be $N = 500$. The symbol $\tilde{\mathbf{B}}$ stands for a low-rank estimate of $\mathbf{B}$ (Andersson et al. 1999). The observation operator for the LOS winds consists of the horizontal interpolation to simulated locations of DWL measurements and a projection operator for different azimuth angles. The calculation of the error statistics was carried out separately for each of the scenarios.

Resulting errors in the physical space are in our model zonally nearly homogeneous and the meridional wind errors are more homogeneous in the y direction than errors in the zonal wind (not shown). Close to the equator, magnitudes of the zonal wind errors at 500-hPa level are somewhat larger than the meridional wind errors because of the impact of the Kelvin waves, which are centered at the equator.

Magnitudes of errors used in the assimilation are amplified (multiplying by a constant factor) with respect to the values derived by the randomization to produce magnitudes of simulated errors which roughly correspond to those expected for the ADM mission (Tan and Andersson 2005). Errors for the Aeolus winds and the component perpendicular to the line of sight of Aeolus are almost equal to the zonal and meridional errors because selected orbit parameters make Aeolus measurements nearly zonal.

Simulated observations for both LOS winds and potential temperature are perturbed by adding them a value from a Gaussian distribution $N(0, \sigma_b)$, where it is assumed that $\sigma_o = \sigma_b$. There is no strong a priori reason for making this choice, but it was suitable for us to use the same weight on observations and the background fields. In any case, the choice made is not significantly important in our study measuring the added value of the second DWL satellite.

Fields generated by the randomization are used also for the preparation of observations. An advantage is that the simulated observations and the background errors will have the same statistics in terms of equatorial waves. This enables a detailed comparison between the value of observations and that of reliable first-guess error information. Magnitudes are scaled so that the errors of the background and observations have magnitudes which are on average about 10% of the magnitudes of simulated observations. In each case, the energy in the simulated truth is dominated by the kinetic energy; potential energy contributes on average about 20% of the total energy. Contributions to the kinetic energy from the zonal and meridional winds are almost equal because the background-error variances derived from the ECMWF fields are characterized by the equipartition of energy in the two components. An ensemble of cases is prepared and 3DVAR and 4DVAR experiments are carried out for five scenarios. This experiment is discussed in the result section as an experiment with "reliable variances and many small scales."

In addition to the "truth" simulated by randomization experiments, monthly mean fields from the ECMWF analyses have also been used. Potential temperature and winds at the 500-hPa level are used as initial states from which the forecasts are run until they adjust to the model, as estimated from the energy partition and energy changes. In order not to lose the meridional component of the flow in our simple model, the forecast model was applied with three major heating sources centered at the equator (representing the three continental areas of the tropics) and a 12-h heating cycle. Solutions obtained in this way were used to create observations. First-guess fields for the assimilation were prepared by averaging the model trajectories over a day and adding some extra noise.

Nature simulations prepared in this way are characterized by a variance whose distribution among various equatorial waves is different from the background-error variance distribution. Therefore, these simulations will be referred to as "unreliable background-error experiments" or experiments with poor background-error covariances. This experiment can be considered to be closer to NWP applications than to the experiment that applies reliable background-error covariances.

For a fairer comparison between the observational and background terms of assimilation, another set of the truth and first-guess fields is prepared in which the above-described fields are projected onto the subspace defined by the background-error covariance matrix and only a projected part of the flow is used to create observations and as a first guess in the assimilation. This experiment will be referred to as a "large-scale mainly zonal flow" experiment.

4. Relative impact assessment of simulated observations

Now we present results of the assimilation for various scenarios with two DWLs. Their impact is discussed with respect to Aeolus and the quality of background-error covariances. As will be shown, the representativeness of the background-error term influences the analysis results to a great extent. In most experiments, 4DVAR results are contrasted to those based on the 3DVAR assimilation.

a. Tropical background-error covariances: An example of an ER wave

To illustrate the impact of the background-error covariances, we use as truth the analytical solution for the equatorial $n = 1$ Rossby wave with the global wavenumber 6, presented in Ž04. An important difference between the two cases is the background-error variance distribution, which is now taken from the ECMWF model level close to 500 hPa.

Compared to the earlier result (Figs. 9 and 10 in Ž04), Fig. 5 illustrates the fact that real forecast errors have small scales and that errors in wind and mass fields at the 500-hPa level in the tropics are coupled only weakly. Thus, the analysis increments obtained by the assimilation of mass-field observations provide almost no information about the wind field close to the equator (Fig. 5b), and the assimilation of LOS winds provides no significant information about the height field (Fig. 5c). However, the assimilation of Aeolus winds, although they are nearly zonal, recovers well the nondivergent flow of the wave (Figs. 5c,d). The meridional wind component, missing from the observations, has been provided through the background-error covariance matrix. The background-error spectrum is dominated by the contribution from the ER waves, especially at large scales, which we observe. In the subtropics, the relative importance of the ER waves further increases compared to at the equator; consequently, the

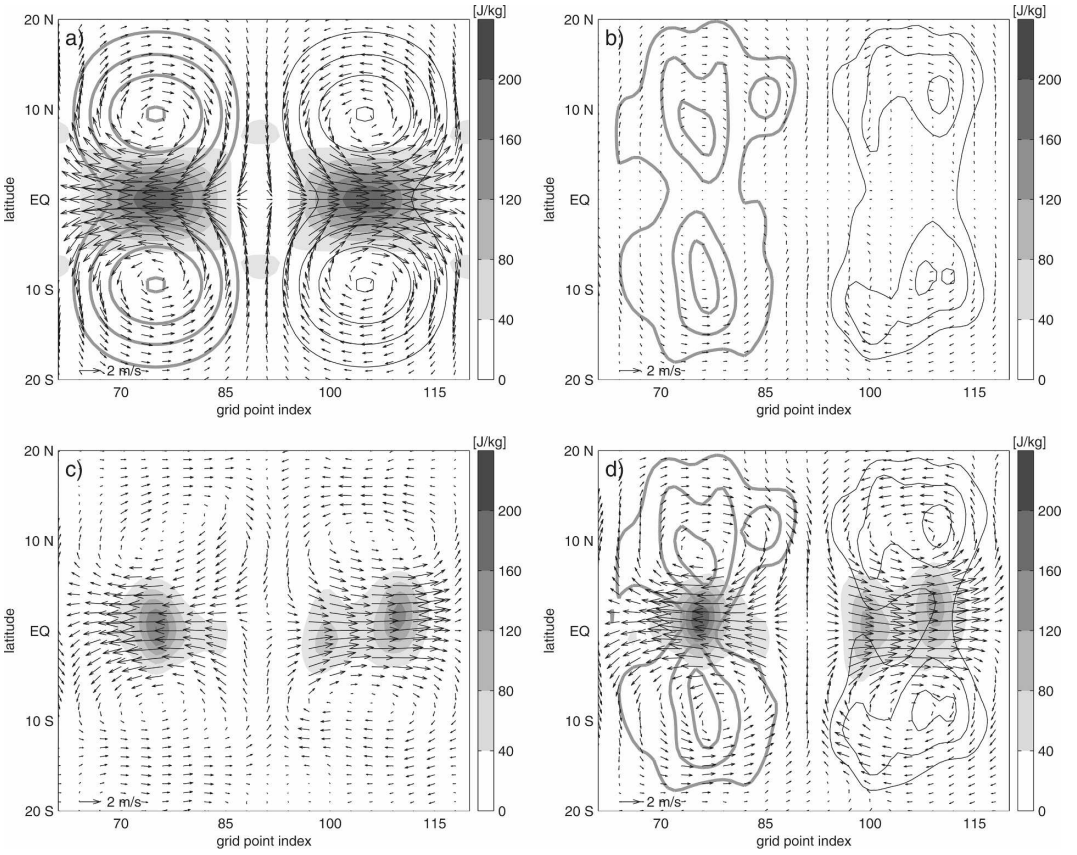

FIG. 5. 3DVAR analysis solution of a single equatorial $n=1$ Rossby wave using observations taken along the ADM-Aeolus track: (a) truth, (b) assimilation of height data, (c) assimilation of Aeolus winds, and (d) assimilation of height observations and Aeolus winds. Error variance is from the model level 39 (spectra shown in Fig. 2). Thick gray (thin black) lines correspond to positive (negative) mass-field perturbation. Shading is used for the kinetic energy with levels of shading indicated in the color bar.

assimilation of height observations was capable of reconstructing a part of the geostrophically balanced wind field off the equator (Fig. 5b). Adding another DWL in this experiment (besides the Aeolus) does not improve the analysis because Aeolus winds have already been sufficient to recover the simulated large-scale pattern.

However, if the background-error spectrum is not dominated by the mass–wind coupling of the ER wave, the assimilation is more sensitive to the type of available LOS measurements. Figure 6 illustrates this sensitivity in the case where the amplitude of EIG and Kelvin modes in the background-error spectrum has been increased at the expense of the ER waves. Winds recovered from height observations in this case have erroneous directions and are predominantly zonal, especially in the subtropics (not shown). When the mass-field observations are complemented by the Aeolus winds, zonal winds of the wave are reconstructed (Fig. 6a), but the meridional component and nondivergent circulation are absent. An improvement obtained by a second satellite is significant in this case. Adding any information about the other wind component, complementing the Aeolus zonal winds, makes a major improvement to the meridional wind (Fig. 6b). On average, analysis results are improved by the second satellite to an extent that depends on its LOS direction with respect to Aeolus, the observation coverage, and the reliability of the background-error term for the analysis.

b. *Idealized flows with known variance and many small scales*

This is the main experiment of the study. The observations represent complex small-scale tropical structures prepared using the background-error matrix, as explained in section 3c.

We start the discussion by comparing 3DVAR analysis increments for various scenarios. Figure 7 shows

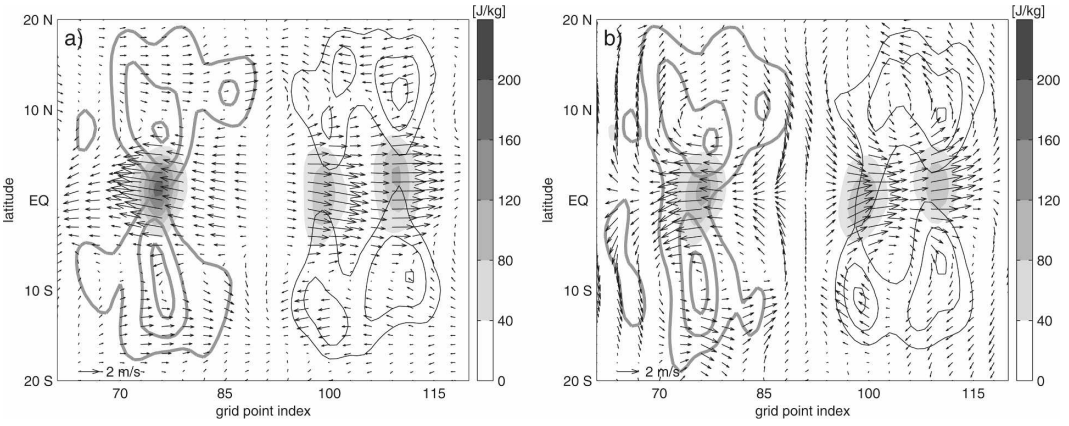

FIG. 6. Same as Fig. 5d, but with unreliable background-error information: (a) Aeolus and (b) reduced dual-perspective scenario.

analysis increments when only LOS winds are assimilated. Observation points are included in the figures and differences between Aeolus and four other scenarios are provided to illustrate the added value of another satellite with respect to Aeolus.

The structure of increments arises from observations and from the background-error term spreading observed information horizontally. It can be seen in Fig. 7 that increments are located along the satellite tracks. Differences between Aeolus and a second satellite show that the added value from the dual-perspective scenarios is mainly in the meridional wind component; the value added by tandem-Aeolus manifests mostly in zonal winds in the neighborhood of the second satellite track. The dual-inclination scenario provides added value about equally in the zonal and meridional wind components. When temperature data are added to LOS winds in 3DVAR, only the mass-field structure is affected.

These features are reflected in the analysis scores, shown in Fig. 8. This figure demonstrates the fact that errors in the mass and wind fields are effectively uncoupled; that is, the assimilation of LOS winds reduces the first-guess error for the temperature field by only a few percent. The same applies to the wind scores and the assimilation of temperature observations. All together, Fig. 8 indicates that our 3DVAR assimilation system behaves as if the analysis were nearly univariate, even though it was formulated as a multivariate method. This result is in line with previously studied sensitivities in the tropics and with the behavior of the full-scale NWP systems.

In the present 3DVAR case, which has reliable background-error statistics, the observation coverage and local LOS direction with respect to the true wind direction are factors that determine the impact of various DWL scenarios. Thus, the observations taken at locations of the tandem-Aeolus scenario provide the best impact for the zonal wind, but the two dual-perspective scenarios are superior in the meridional wind scores. The dual-inclination scenario is between these two options for the wind field; at the same time, it provides the best scores for temperature because of its coverage and relatively more data (Fig. 8). Relative improvements from the various scenarios with respect to Aeolus range between zero and 20%. The lack of added value from the dual-perspective and reduced dual-perspective scenarios to the temperature and zonal wind scores reflects both the fact that the spatial coverage for these scenarios is nearly the same as for Aeolus and the inefficiency of mass–wind and wind–wind couplings available in the background-error covariance matrix.

When 4DVAR is employed instead of 3DVAR, each observation is taken into account at its appropriate time and the model is used to propagate observed information back and forth in time (Thépaut et al. 1996). In this way the missing wind component can be extracted with the help of the dynamics of the model equations and background-error covariances. A difference between the impact of assimilating LOS winds alone or together with temperature observations becomes significant, although results are not necessarily better (Fig. 9 versus Fig. 8). The 4DVAR scores shown in Fig. 9 are valid for the end of the 12-h assimilation window and 3DVAR was performed for the same time instant, meaning that the truth is the same in the two cases, but the first guess is not.

Assimilation of only temperature observations in 4DVAR makes the zonal wind scores worse than in 3DVAR case; moreover, analysis scores are worse than those of the first-guess field in cases of the Aeolus and dual-perspective scenarios. This is in contrast to the

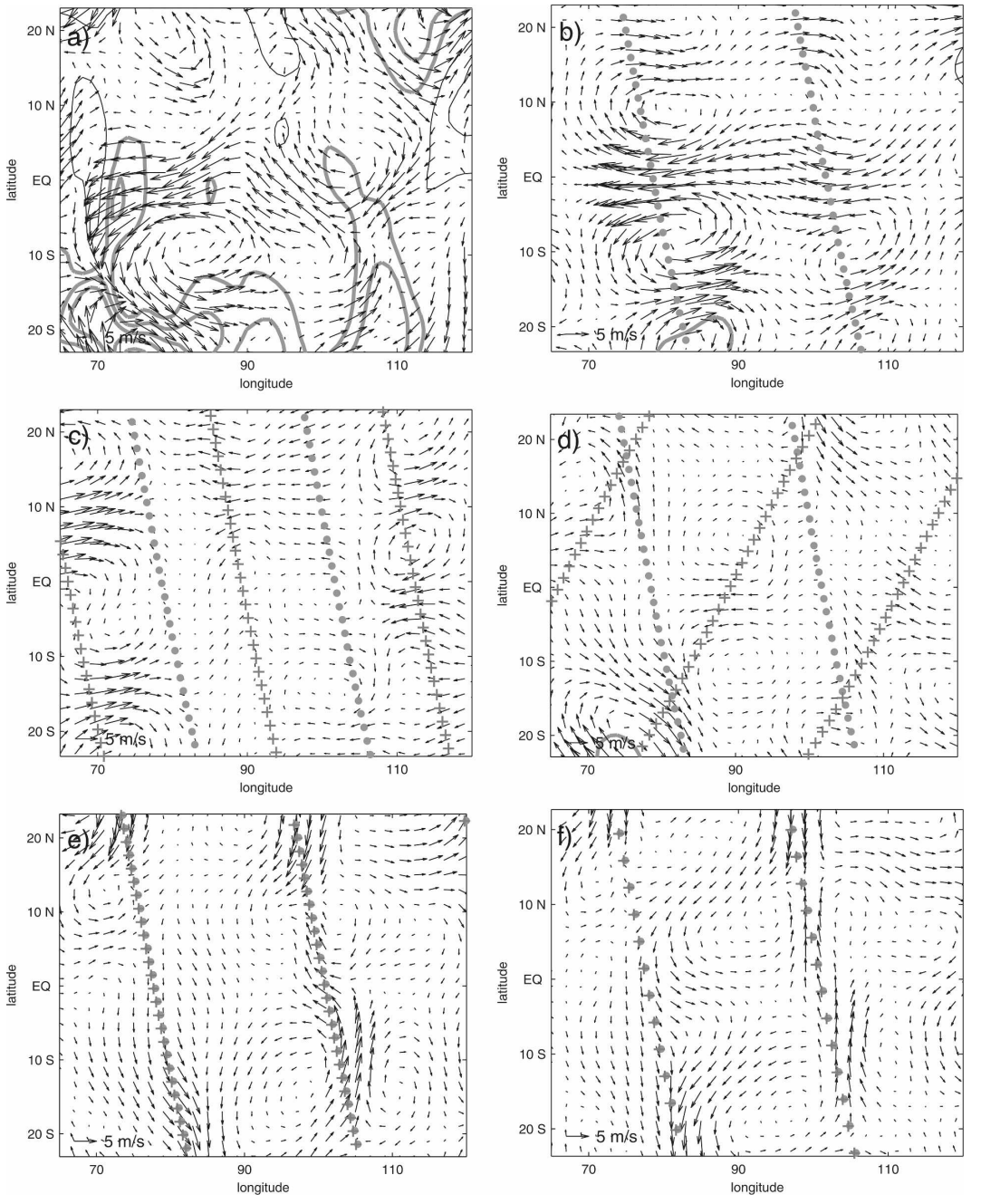

FIG. 7. Examples of 3DVAR analysis increments due to LOS winds: (a) "true" increments ("nature" first-guess field), (b) analysis increments obtained by 3DVAR assimilation of LOS winds at observation locations simulated for Aeolus, and differences in increments between scenarios with two satellites and Aeolus, namely, the (c) tandem-Aeolus–Aeolus, (d) dual-inclination–Aeolus, (e) dual-perspective–Aeolus, and (f) reduced dual-perspective–Aeolus scenarios. Thick gray (thin black) lines correspond to positive (negative) potential temperature increments, with spacing every 1 K. Gray circles correspond to measurement positions of Aeolus; pluses denote positions of a second satellite.

results presented in Fig. 12 in Ž04, where 4DVAR always improved over 3DVAR when covariances were reliable. The difference is in the amount of inertio-gravity waves (i.e., flow divergence), which is much larger in the present simulations; also, the flow is more nonlinear. This makes the internal adjustment process in 4DVAR complex and inefficient, in contrast to the earlier study where 4DVAR was able to extract useful

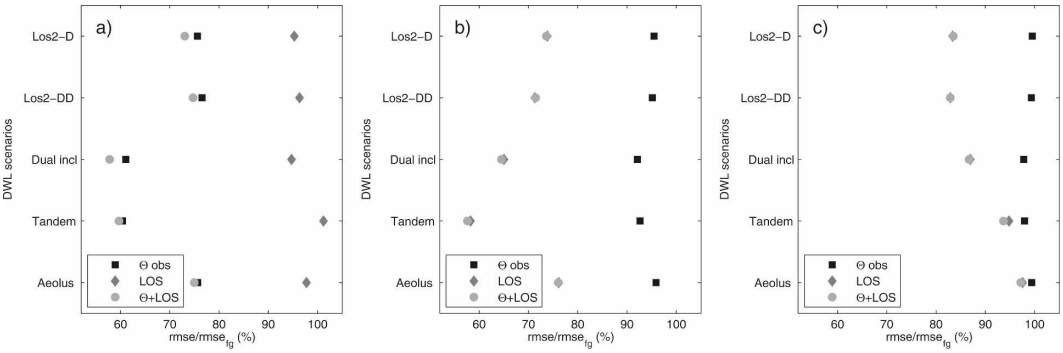

FIG. 8. Analysis errors (rmses) for various scenarios, observation types, and variables in 3DVAR assimilation and an ensemble of experiments with complex tropical small-scale flows. Rmse for (a) potential temperature, (b) zonal wind, and (c) meridional wind. Various symbols denote observation types used in assimilation, as indicated in the legend.

information about the wind field from the mass data. Furthermore, simulated flow is dominated by small scales, which are poorly observed in dual-perspective scenarios.

The recovery of the meridional wind component is better with respect to 3DVAR for the tandem-Aeolus and the dual-inclination scenarios (Fig. 9c). The latter is now superior to the dual-perspective scenarios and it provides, on average, the best analysis scores, followed by the tandem-Aeolus (for u wind) and dual-perspective (for v wind) scenarios.

Together, good performance of the reduced dual-perspective scenario in comparison to the dual-perspective scenario, and relatively better scores for the tandem-Aeolus and dual-inclination scenarios illustrate the importance of the observation coverage in the zonal direction. Many motions in the tropics either propagate vertically or are channeled along the equatorial waveguide and cannot propagate out of the tropics; thus, good observational coverage in the zonal direction is important. Here, it can also be noted that the assimilation is dominated by the wind data, and corrections to the first-guess temperature field during minimization are always small and energetically much less important than corrections made to the wind field.

The analysis increments from 4DVAR are illustrated in Fig. 10 for the assimilation of temperature data and LOS winds together. The verifying structure is shown in Fig. 7a. Figure 10 illustrates that in spite of the perfect-model assumption and a reliable background-error term for the analysis, nearly zonal LOS winds from Aeolus are not sufficient to recover the flow structure off the track and in the meridional direction. Improved coverage is provided by the tandem-Aeolus scenario, but the dual-inclination scenario appears more advantageous because it provides not only a larger amount of observations but also some information about the meridional component. In conclusion, for complex tropical flows with approximately equal kinetic energy partition between the zonal and meridional wind and with a reliable background-error term, the results suggest that the dual-inclination scenario would be preferable to the tandem-Aeolus and dual-perspective scenarios in the tropics.

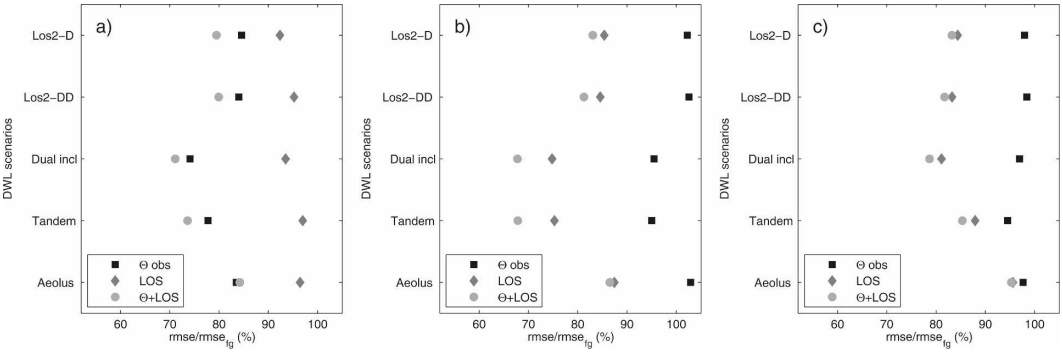

FIG. 9. Same as Fig. 8, but for 4DVAR assimilation.

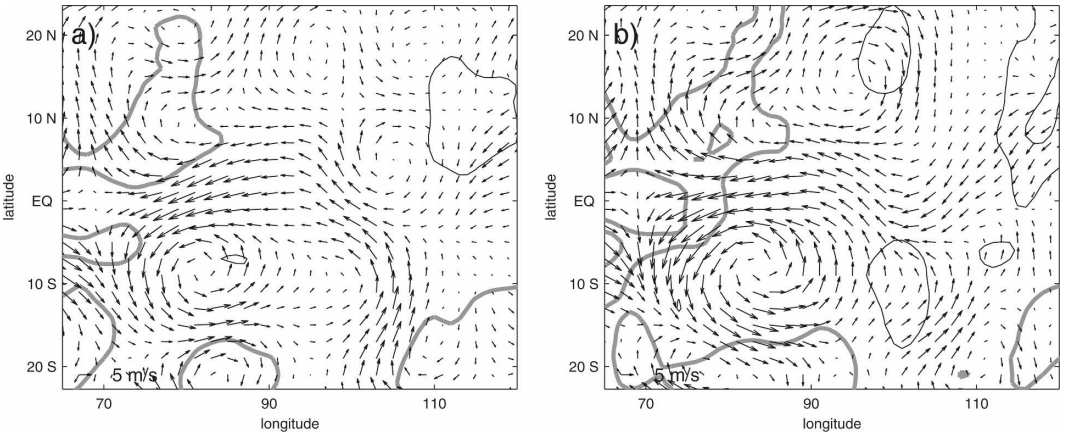

FIG. 10. 4DVAR analysis increments at the end of the 12-h assimilation window from temperature and LOS wind observations for the (a) Aeolus and (b) dual-inclination scenarios.

c. *Large-scale mainly zonal flow*

In the predominantly zonal-flow case it can be expected that the tandem-Aeolus scenario will perform better with respect to dual-perspective scenarios than in the previous experiment with u and v components equally important. This experiment aims at quantifying the difference. It is especially interesting for a comparison with PIEW, where it was concluded that the tandem-Aeolus scenario provides a better impact on average than the other two scenarios in the midlatitudes.

As explained in section 3c, observations are obtained in this case from the average tropical circulation at 500 hPa adjusted to the present model and projected onto the equatorial waves present in the background-error covariance matrix. Zonal winds dominate; over 80% of the kinetic energy is in the zonal wind component and about the same percentage of the total energy is kinetic energy. The flow is smooth and dominated by structures which have large scales. In the subtropics, perturbations in the mass field are more significant and geostrophically balanced with the wind field.

In this experiment the variance of the simulated model atmosphere is not distributed among the various equatorial modes in exactly the same proportions as in the background-error matrix (which was the case for the previous experiment where u and v components were equally important). This means that the background-error statistics, although they support observations, are not useful to the extent they were earlier.

As previously, in 3DVAR assimilation the tandem-Aeolus scenario performs best for the zonal wind, and the dual-perspective scenario is most successful in reducing the errors in the meridional wind (Fig. 11). The added value of the second satellite in 3DVAR ranges from a few percentages up to about 25% for the meridional wind component and dual-perspective scenarios. The reduced dual-perspective scenario is almost as good as the dual-perspective because the assimilated

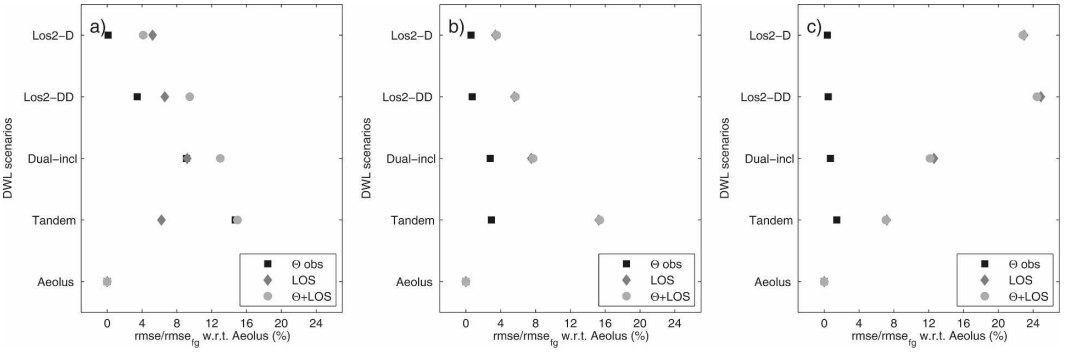

FIG. 11. Same as Fig. 8, but for the large-scale flow experiment. Reductions of the first-guess errors for various scenarios and observation types are shown relative to those for Aeolus (i.e., the value added by the second DWL is shown).

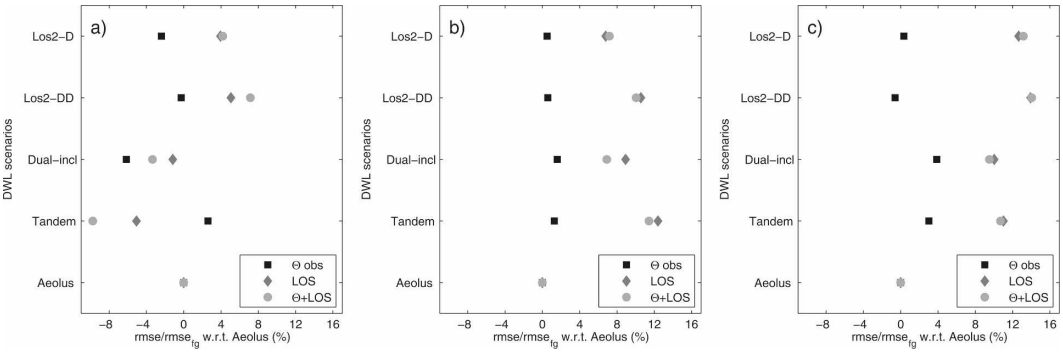

FIG. 12. Same as Fig. 11, but for 4DVAR assimilation.

meridional structures are large. However, because the meridional component makes up a smaller part of the total flow, the relative improvement is dominated by the value added by the tandem-Aeolus scenario to the zonal wind analysis.

Compared to the 3DVAR case, where the added value of another satellite is always positive, in the 4DVAR case temperature scores become worse with more observations, especially for the tandem-Aeolus and dual-inclination scenarios (Fig. 12a). Possible reasons can be found in the simplicity of our model and in the way the experiment was prepared. Our assimilation system produces analysis fields that contain significant amounts of divergence. However, the model itself does not contain a physical process that would maintain or generate the divergence. Therefore, during the model integration in 4DVAR, some useful divergence information obtained from the mass data is lost by its adjustment to the wind field and background-error covariances. In addition, it is possible that the fields, which served as truth, were not entirely balanced after they were projected onto the subspace of the background-error covariance matrix and an adjustment process during 4DVAR removed a part of the useful temperature information from the data. It is also possible that observations include more geostrophically balanced information, especially in the subtropics, than is present in the background-error covariance matrix. This difference can also be a reason why the dual-perspective scenario, which provides the vector wind information, has a somewhat greater value than the dual-inclination scenario.

The background-error reduction in 3DVAR is between 5% and 50%, depending on the observation type and the variable verified (not shown). The smallest improvement is for the unobserved variable (temperature in the case of LOS data and wind variables in cases where temperature observations are assimilated). Adding temperature observations to LOS winds does not improve the scores for wind components in any scenario, illustrating once again the inefficiency of the average mixture of multivariate relationships for the tropical variational assimilation. Major improvements occur for the meridional wind in 4DVAR with respect to 3DVAR; the root-mean-square error of the first-guess field is reduced in all scenarios by an additional 20%–30% in comparison with 3DVAR, where the reduction was significant only for the dual-perspective scenarios (not shown). An example of 4DVAR increments shown in Fig. 13 illustrates the ability of 4DVAR to recover the unobserved meridional flow in the Aeolus, tandem-Aeolus, and dual-inclination scenarios.

If the background-error covariances represent the observed flow poorly, adding another satellite results in a much greater benefit for the analysis than in the previous cases. This is illustrated in Fig. 14 with experiments using the nature and first-guess fields as in the previous experiment but without projection onto the modes of the background-error matrix. In addition, the background-error statistics are somewhat different, with more weight given to small-scale structures and to the Kelvin and inertio-gravity motions. 4DVAR analysis scores from this experiment are shown in Fig. 14 and can be contrasted with those in Fig. 12.

A comparison of the two figures shows that the improvements with respect to Aeolus can be 2–3 times larger depending on the reliability of the background-error covariances. In case of poor covariances, the added value of another satellite can be larger than 40% of the first-guess error. The tandem-Aeolus scenario is now slightly outperformed by both the dual-perspective and dual-inclination scenarios for the zonal wind scores. The reduced dual-perspective scenario provides better results for the meridional wind component than the dual-inclination and tandem-Aeolus scenarios. This result illustrates the value of any information provided about another wind component when the background-

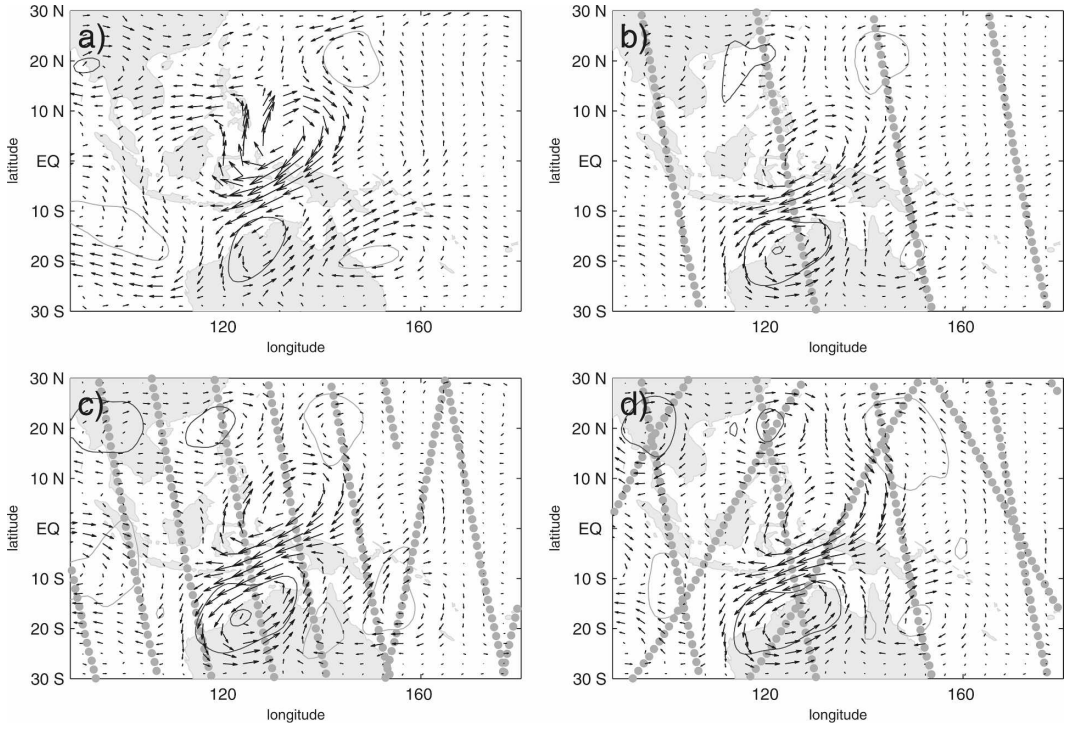

FIG. 13. Same as Fig. 10, but for an example of large-scale tropical flow: (a) truth, (b) Aeolus, (c) tandem-Aeolus, and (d) dual-inclination scenarios.

error information is unreliable, as is the case in NWP applications.

5. Discussion

The presented results highlight the uncertainties of OSSE results related to the background term as used in variational data assimilation and call for further research about the properties of the background-error covariances and their flow dependency in the tropics. We showed here that the reconstruction of the wind vector from a single-perspective LOS component is sensitive to the background-error modeling in the data assimilation system used. As a consequence, the impact of LOS winds can significantly vary with the specification of the background-error term [see, e.g., comments by Stoffelen et al. (2005a) on Riishøjgaard et al. (2004)].

The idealized framework prevents us from comparing directly these results with the results of PIEW. However, the present results suggest that the optimal combination of two DWLs in the tropics is not necessarily the same as in the case of the midlatitudes (tandem-Aeolus). The reason for this difference is the structure of the background-error covariances and the tropical dynamics as compared to the midlatitudes. In

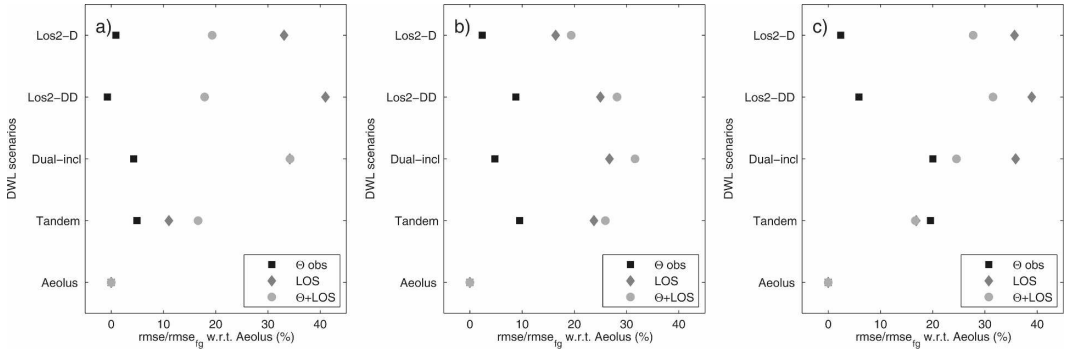

FIG. 14. Same as Fig. 12, but the assimilation uses poor background-error covariances.

particular, the 3DVAR results were illustrative of the difficulty of making use of the balance relationships in the tropics. In spite of the assumed mass–wind coupling in terms of the equatorial waves, the 3DVAR analysis was basically univariate. In this case, the observation coverage and the flow structure determine the added value of the second DWL; that is, the balance relationships did not help much in recovering the missing meridional wind component from the mass data and the nearly zonal winds, as measured by the tandem-Aeolus scenario. In the midlatitudes, to the contrary, the geostrophic balance is valid and it effectively extracts the unobserved variables from available observations.

The importance of having some information about the other component increases as the quality of background-error covariances deteriorates and horizontal scales become smaller. Consequently, the added value of another satellite in some cases is an improvement of over 40% with respect to Aeolus in the reduction of the errors in the first-guess fields. Because the numbers obtained apply to the idealized model, it is difficult to translate their values to NWP. It also has to be pointed out that the efficiency of the model dynamics in 4DVAR in the present experiments is related to the perfect-model assumption and the model simplicity.

For a realistic assessment of proposed follow-on ADM missions in NWP, global OSSE experiments with a state-of-the-art NWP model are needed. Although it is unknown what the assimilation system (and partly also the observing system) would be 10 or more years in the future, such estimates are good indicators of expected impact. For the ADM-Aeolus, the reduction of analysis and forecasts errors in the ECMWF model in the tropics has been estimated to be of the same magnitude as that produced by radio soundings (Tan et al. 2007). This result is in line with the dynamical arguments about the greater importance of the wind field then the mass field for 4DVAR in the tropics, and it provides a strong motivation for early follow-on missions.

The identical twin OSSE methodology as employed here tends to overestimate the impact of sparse data (Atlas 1997). Another reason for too optimistic results with the simple model in the tropics is the lack of clouds. To evaluate this, we carried out several experiments in which the role of clouds was simulated by leaving holes in the data. The scores were made worse to an extent proportional to the amount of observations removed in various scenarios while the relative value of various scenarios with respect to ADM-Aeolus remained the same.

Furthermore, a more realistic study should also consider wind vectors derived from cloud motions. These observations have impact in the tropics in most data assimilation systems. However, the background-error covariance matrix tends to be vertically shallow while the cloud-motion winds are provided on a few levels at most. There are problems with height assignments, and horizontally correlated height errors seriously compromise the quality of derived wind. But cloud-motion winds still have significant impact because tropical wind analyses are otherwise rather poor. With both cloud-motion and Aeolus winds available, the LOS wind profiles could be very useful in improving the assimilation of cloud-drift wind data.

This study was based on the idea that the ADM-Aeolus mission would be successful and that any follow-on mission will be a combination of two DWL instruments of the Aeolus type.

Extensive work has been ongoing to evaluate other DWL concepts, especially scanning DWLs (e.g., Masutani et al. 2006, and references therein). In particular, Masutani et al. (2006) show by performing OSSE experiments using the NWP model of the National Centers for Environmental Prediction that the scanning (wind vector observations) is most important in the upper troposphere of the tropics and that the scanning DWL always outperforms the nonscanning instrument.

The results presented were obtained by using the background-error variances representative for the midtroposphere. However, there is a possibility for large improvements in stratospheric wind analyses and the related transport of constituents in the middle atmosphere by providing global observations of wind profiles (Polavarapu et al. 2005). On the other hand, a significant improvement of the tropical stratospheric winds has been demonstrated by Gaspari et al. (2006), based on improved modeling of the background covariance functions. For the evaluation of DWL scenarios in the tropical stratosphere, two aspects are particularly interesting. First, the meridional wind component is less important in the tropical stratosphere than in the troposphere. Second, according to the more recent analysis of the tropical forecast errors, mass–wind coupling in the tropical stratosphere is stronger than in the troposphere, and this coupling is stronger during the negative phase of the quasi-biennial oscillation (Žagar et al. 2007). Both aspects are likely to provide dynamical arguments relevant for the planning of future spaceborne DWL missions.

6. Summary and conclusions

This study compares dynamical aspects of the assimilation of spaceborne wind observations from several

recently proposed scenarios with two Doppler wind lidars (DWLs) in space. The impact is measured with respect to ADM-Aeolus, a DWL satellite built by the European Space Agency with launch scheduled for 2009. The scenarios include a tandem-Aeolus with two satellites in one orbit plane with a 180° phase difference, two satellites in orbits with different inclination angles, and two satellites in the ADM-Aeolus orbit providing the complete wind vector. All scenarios considered are assumed to use the same Aeolus instrument.

DWL measurements by ADM-Aeolus provide horizontal line-of-sight (LOS) wind components. In the tropics, observed LOS winds are nearly zonal; thus, the meridional flow is inferred from the background flow, the assumed structures of the background-error covariances, and the model dynamics in 4DVAR. Another satellite measuring additional LOS component additionally increases the value of the analysis fields depending on its observation coverage, the direction of the second LOS measurement with respect to Aeolus, the flow properties, and the data assimilation modeling.

The model used for the assimilation solves three nonlinear equations for potential temperature and two wind components that describe the horizontal structure of these fields in regions of deep tropical convection. Although highly simplified with respect to NWP models, the model applies the realistic horizontal representation of forecast errors in the tropics, and it is thus suitable for studying the dependence of the assimilated horizontal structures of equatorial waves on background information in the data assimilation system.

Assimilation experiments were carried out by applying three- and four-dimensional variational methods to simulated temperature and LOS wind observations. The results suggest that the optimal choice among the three scenarios proposed by the PIEW project (Marseille et al. 2008) is not necessarily the same one as in the case of the midlatitudes (i.e., tandem-Aeolus). The most likely reason for the difference is the structure of the tropical background-error covariances, that is, differences in the dynamics of the tropics as compared to those of the midlatitudes.

The results of 3DVAR assimilation illustrate the inefficiency of multivariate data assimilation in the tropics. It is shown that, in spite of the assumed balance relationships in terms of the linear equatorial waves, the 3DVAR results make it appear as if mass–wind coupling did not occur. The consequence for the assimilation of LOS winds is that the missing part of the wind vector cannot be reconstructed from the mass-field observations and applied balances as in the case of the midlatitudes.

Under the conditions of reliable background-error statistics, large-scale flow, and a perfect model in 4DVAR, the differences among various scenarios are not large. As the horizontal scales become smaller and the flow becomes less zonal, the importance of having information about the other wind components (i.e., the vector wind) increases. The added value of another DWL satellite with respect to Aeolus varies between 0% and 40%, depending on the quality of the background-error covariances, the observation type, and the variable verified.

Acknowledgments. The authors thank Chris Snyder and Joe Tribbia (NCAR) for reading the manuscript and providing helpful comments, and to Erland Källén (MISU) for his contribution to the discussions of the project. This study was funded via EUMETSAT Contract EUM/CO/05/1447/PS, project "DWL sampling scenarios."

REFERENCES

Andersson, E., M. Fisher, R. Munro, and A. McNally, 1999: Diagnosis of background errors for radiances and other observed quantities in a variational data assimilation scheme, and the explanation of a case of poor convergence. *Quart. J. Roy. Meteor. Soc.,* **126,** 1455–1472.

Atlas, R., 1997: Atmospheric observations and experiments to assess their usefulness in data assimilation. *J. Meteor. Soc. Japan,* **75,** 111–130.

Baker, W., and Coauthors, 1995: Lidar-measured winds from space: A key component for weather and climate prediction. *Bull. Amer. Meteor. Soc.,* **76,** 869–888.

Daley, R., 1993: Atmospheric data analysis on the equatorial beta plane. *Atmos.–Ocean,* **31,** 421–450.

Davey, M. K., 1989: A simple tropical moist model applied to the '40-day' wave. *Quart. J. Roy. Meteor. Soc.,* **115,** 1071–1107.

——, and A. E. Gill, 1987: Experiments on tropical circulation with a simple moist model. *Quart. J. Roy. Meteor. Soc.,* **113,** 1237–1269.

Ferranti, L., T. N. Palmer, F. Molteni, and E. Klinker, 1990: Tropical–extratropical interaction associated with the 30–60 day oscillation and its impact on medium and extended range prediction. *J. Atmos. Sci.,* **47,** 2177–2199.

Fisher, M., 2003: Background error covariance modelling. *Proc. ECMWF Seminar on Recent Developments in Data Assimilation for Atmosphere and Ocean,* Reading, United Kingdom, ECMWF, 45–64.

——, and P. Courtier, 1995: Estimating the variance matrices of analysis and forecast errors in variational data assimilation. ECMWF Tech. Memo. 220, 28 pp.

Gaspari, G., S. E. Cohn, J. Guo, and S. Pawson, 2006: Construction and application of covariance functions with variable length fields. *Quart. J. Roy. Meteor. Soc.,* **132,** 1815–1838.

Gill, A. E., 1980: Some simple solutions for heat-induced tropical circulation. *Quart. J. Roy. Meteor. Soc.,* **106,** 447–462.

——, 1982: Studies of moisture effect in simple atmospheric mod-

els: The stable case. *Geophys. Astrophys. Fluid Dyn.,* **19,** 119–152.

Gordon, C. T., L. Umscheid, and K. Miyakoda, 1972: Simulation experiments for determining wind data requirements in the tropics. *J. Atmos. Sci.,* **29,** 1064–1075.

Heckley, W. A., and A. E. Gill, 1984: Some simple analytical solutions to the problem of forced equatorial long waves. *Quart. J. Roy. Meteor. Soc.,* **110,** 203–217.

Kistler, R., and Coauthors, 2001: The NCEP–NCAR 50-Year Reanalysis: Monthly means CD-ROM and documentation. *Bull. Amer. Meteor. Soc.,* **82,** 247–267.

Lorenc, A. C., 2003: Modelling of error covariances by 4DVAR data assimilation. *Quart. J. Roy. Meteor. Soc.,* **129,** 3167–3182.

Marseille, G.-J., A. Stoffelen, and J. Barkmeijer, 2008: Impact assessment of prospective space-borne Doppler wind lidar observation scenarios. *Tellus,* **60A,** 234–248.

Masutani, M., and Coauthors, 2006: Observing system simulation experiments at NCEP. NCEP Office Note No. 451, 34 pp.

Matsuno, T., 1966: Quasi-geostrophic motions in the equatorial area. *J. Meteor. Soc. Japan,* **44,** 25–42.

Polavarapu, S., T. Shepherd, Y. Rochon, and S. Ren, 2005: Some challenges of middle atmosphere data assimilation. *Quart. J. Roy. Meteor. Soc.,* **131,** 3513–3527.

Rabier, F., 2005: Overview of global data assimilation developments in numerical weather-prediction centres. *Quart. J. Roy. Meteor. Soc.,* **131,** 3215–3233.

Riishøjgaard, L. P., R. Atlas, and G. D. Emmitt, 2004: The impact of Doppler lidar wind observations on a single-level meteorological analysis. *J. Appl. Meteor.,* **43,** 810–820.

Stoffelen, A., G.-J. Marseille, E. Andersson, and D. H. G. Tan, 2005a: Comments on "The impact of Doppler lidar wind observations on a single-level meteorological analysis." *J. Appl. Meteor.,* **44,** 1276–1277.

——, and Coauthors, 2005b: The atmospheric dynamics mission for global wind measurement. *Bull. Amer. Meteor. Soc.,* **86,** 73–87.

Tan, D. G. H., and E. Andersson, 2005: Simulation of the yield and accuracy of wind profile measurements from the Atmospheric Dynamic Mission (ADM-Aeolus). *Quart. J. Roy. Meteor. Soc.,* **131,** 1737–1757.

——, ——, M. Fisher, and L. Isaksen, 2007: Observing-system impact assessment using a data assimilation ensemble technique: Application to the ADM-Aeolus wind profiling mission. *Quart. J. Roy. Meteor. Soc.,* **133,** 381–390.

Thépaut, J.-N., P. Courtier, G. Belaud, and G. Lemaitre, 1996: Dynamical structure functions in a four-dimensional variational assimilation: A case study. *Quart. J. Roy. Meteor. Soc.,* **122,** 535–561.

Wheeler, M., and G. N. Kiladis, 1999: Convectively coupled equatorial waves: Analysis of clouds and temperature in the wavenumber–frequency domain. *J. Atmos. Sci.,* **56,** 374–399.

World Meteorological Organization, 2000: Statement of guidance regarding how well satellite capabilities meet WMO user requirements in several application areas. WMO Satellite Rep. SAT-22, WMO/TD 992, 29 pp.

Žagar, N., 2004: Assimilation of equatorial waves by line-of-sight wind observations. *J. Atmos. Sci.,* **61,** 1877–1893.

——, N. Gustafsson, and E. Källén, 2004a: Dynamical response of equatorial waves in four-dimensional variational data assimilation. *Tellus,* **56A,** 29–46.

——, ——, and ——, 2004b: Variational data assimilation in the tropics: The impact of a background error constraint. *Quart. J. Roy. Meteor. Soc.,* **130,** 103–125.

——, E. Andersson, and M. Fisher, 2005: Balanced tropical data assimilation based on a study of equatorial waves in ECMWF short-range forecast errors. *Quart. J. Roy. Meteor. Soc.,* **131,** 987–1011.

——, ——, ——, and A. Untch, 2007: Influence of the quasi-biennial oscillation on the ECMWF model short-range forecast errors in the tropical stratosphere. *Quart. J. Roy. Meteor. Soc.,* **133,** 1843–1853.